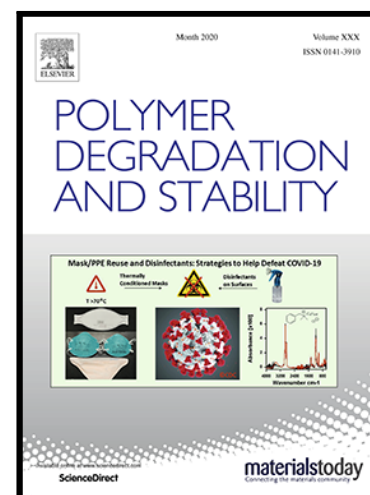# Journal Pre-proof

Bismaleimide resins modified by an allyl ether of bio-based resveratrol with excellent halogen-free and phosphorus-free intrinsic flame retardancy and ultrahigh glass transition temperature

Zilong Zhang , Xiaohan Li , Ying Bao ,
Wei Wei Writing - review & editing , Xiaojie Li Supervision ,
Xiaoya Liu Supervision

Please cite this article as: Zilong Zhang , Xiaohan Li , Ying Bao , Wei Wei Writing - review & editing , Xiaojie Li Supervision , Xiaoya Liu Supervision , Bismaleimide resins modified by an allyl ether of bio-based resveratrol with excellent halogen-free and phosphorus-free intrinsic flame retardancy and ultrahigh glass transition temperature, *Polymer Degradation and Stability* (2021), doi: https://doi.org/10.1016/j.polymdegradstab.2021.109717

Bismaleimide resins modified by an allyl ether of bio-based resveratrol with excellent halogen-free and phosphorus-free intrinsic flame retardancy and ultrahigh glass transition temperature

Zilong Zhang, Xiaohan Li, Ying Bao, Wei Wei[*], Xiaojie Li, and Xiaoya Liu

School of Chemical and Material Engineering, Jiangnan University, Wuxi, Jiangsu 214122, P. R. China

[*]Corresponding author: Wei Wei (E-mail: wwei1985@jiangnan.edu.cn)

Abstract

Development of new allyl compounds to modify bismaleimide (BMI) resins for improving the toughness while maintaining a high thermal performance and flame retardancy is still urgent. In this study, we synthesized the allyl ether of resveratrol (AER), a bio-based allyl compound, to modify BMI resin. A series of BMI/AER resins (BA resins) were prepared by changing the molar ratio of BMI to AER. Compared with 2,2'-diallyl bisphenol A (DBA) modified BMI resins (BD resins), which has been widely used in industry, BA resins can be cured at a lower temperature. Although the toughness of cured BA resins was slightly inferior than that of cured BD resins, the cured BA resins exhibited much superior thermal performance and flame retardancy to the cured BD resins. For the BA-0.8 resin with a molar ratio of imide to allyl groups of 1:0.8, the glass transition temperature, thermal decomposition temperature of 5% weight loss, and char yield of the cured product were as high as 388 °C, 415 °C, and

48.6%, respectively. Meanwhile, the UL-94 and limit oxygen index (LOI) tests

revealed an excellent flame retardancy of the cured BA-0.8 resin with V-0 level and

LOI of 37.7%. The remarkable properties were attributed to AER with the

tri-functionality and stiffness conjugated stilbene backbone giving the cured resins

higher crosslinking density, chain rigidity and thermostability compared with DBA.

This work provides a novel insight into the development of high-performance

bismaleimide-based thermosetting resins with excellent halogen-free and

phosphorus-free intrinsic flame retardancy.

Keywords

resveratrol; bismaleimide resins; high thermal stability; high T_g; flame retardancy

Introduction

Bismaleimide (BMI) resin, as a typical thermosetting resin, is a kind of resin

system derived from polyimide resin.[1-4] It is a bifunctional compound with

maleimide ring as active groups, that usually contains multiple aryl groups to enhance

the properties of its cured products. The cured resin has a highly crosslinked network,

which gives it high heat resistance and excellent mechanical properties.[5-7] It is

widely used as matrix materials in cutting-edge fields such as aerospace,[8-10]

microelectronics,[11, 12] and new energy.[13] However, the crosslinking density of

the cured product of unmodified BMI resin is very high, which makes the materials

have the disadvantages of high brittleness and poor toughness.[14] Moreover, BMI

monomer usually has a high melting point and narrow processing window,[15] which

greatly limits its application. Therefore, the modification of BMI resin has become the

key to the preparation of high-performance BMI thermosets.

As for academic research and industrial development, most of the modification of

BMI resin is based on the combination of BMI with allyl compounds, in which

2,2'-diallyl bisphenol A (DBA) is the most successful modifier.[16] BMI/DBA system

(BD resin) provides linear chain extension through the ene reaction, and Diels-Alder

(D-A) reaction occurs at high temperature.[17] Then the final network has excellent

toughness and thermal properties. However, the production of DBA is very dependent

on bisphenol A derived from petroleum resources.[18] Studies have shown that

bisphenol A, with a structure similar to that of estrogen, may make the human body

more susceptible to diseases, reduce fertility and lead to a variety of cancers.[19] In

addition, with the rapid development of science and technology (and industry), the

working environment of materials is increasingly strict, especially in aerospace,

electrical, communications and other cutting-edge fields. The demand for

high-performance resin with high temperature resistance and flame retardancy is

increasingly urgent. But BMI/DBA system will reduce the flame retardancy of

bismaleimide resin,[20] which limits the application of bismaleimide resin in

cutting-edge fields.

Resveratrol can be easily extracted from grape, polygonum cuspidatum and

peanuts,[21-23] and its structure has a feature that three phenolic hydroxyl groups

surround the framework of stilbene. As a bio-based resource, resveratrol has potential benefits to human health,[24] and its special structure makes it an ideal raw material for preparation of polymer materials, especially thermosetting resin. Cash et al.[25] synthesized a resveratrol-based cyanate resin. Compared with bisphenol A cyanate resins, the resveratrol-based cyanate resins showed higher glass transition temperature (T_g) and significantly increased char yield. Zhang et al.[26, 27] synthesized several completely bio-based trifunctional benzoxazine resins from resveratrol. These resveratrol-based benzoxazine resins presented high thermal performance, and the flame retardancy test showed that these were all self-extinguishing and nonflammable materials. The resveratrol-based three functional epoxy resin (REEP) was synthesized by Tian et al.[28] The resveratrol-based epoxy/methyl hexahydrophthalic anhydride (REEP/MeHHPA) resin had high thermal properties, superb tensile properties, excellent dielectric properties and low flammability. Fang et al.[29-31] successfully prepared propargyl ether resin, organic fluorine resin and benzocyclobutene resin from resveratrol. These novel resveratrol-based thermosetting resins showed excellent properties such as high heat resistance, low coefficient of thermal expansion and excellent hydrophobicity. The above researches show that resveratrol has great potential applications in the synthesis and modification of thermosetting resins, especially in improving thermal performance and flame retardancy. In consideration of the advantages of resveratrol, it is attractive to develop new and high-performance thermosetting resin by combining resveratrol with bismaleimide.

In this study, allyl ether of resveratrol (AER) was synthesized with bio-based resveratrol as raw material, and used to modify BMI resin. A series of BMI/AER resins (BA resins) were prepared by changing the molar ratio of BMI to AER. The thermal curing behavior of BA resins, as well as the mechanical properties, thermal performance, and flame retardancy of cured products, were comprehensively studied and compared with those of BD resins, which has been widely used in industry. It was found that the BA resins exhibited superior thermal properties (higher T_g and significantly improved char yield) and halogen-free and phosphorus-free inherent flame retardancy to those of BD resins, indicating its bright application prospects as a high-performance thermosetting resin.

Experimental

Materials

Resveratrol (RES, >99%), allyl bromide (>98%), anhydrous potassium carbonate (K$_2$CO$_3$, AR), and 4,4'-bismaleimidodiphenylmethane (BMI, >96%) were purchased from Shanghai Aladdin Bio-Chem Technology Co. Ltd. *N,N*-Dimethylformamide (DMF, AR) and dichloromethane (DCM, AR) were supplied by Shanghai Titan Technology Co., Ltd. 2,2'-Diallyl bisphenol A (DBA, >90%) was purchased from Shanghai Macklin Biochemical Technology Co., Ltd. Deionized water was obtained from School of Chemistry and Materials Engineering, Jiangnan University.

Synthesis of AER

First, RES (13.0 g, 56 mmol), anhydrous K_2CO_3 (38.7 g, 280 mmol) and DMF

(150 mL) were mixed with stirring under N_2 atmosphere, and then allyl bromide (34.6

g, 280 mmol) was added dropwise. Then the mixture was stirred at 80 °C for 10 h.

After the end of the reaction, the excessive allyl bromide and most of DMF were

removed by rotary evaporation. Next, the concentrated product was dropped into

deionized water and continuously stirred to disperse, and then extracted with DCM.

Last the organic layer was concentrated by rotary evaporation, washed with deionized

water for several times, and finally dried in vacuum overnight. The yield was 74.3%.

^{1}H-NMR (400 MHz, CDCl$_3$) δ (ppm): 7.47 – 7.40 (m, 2H), 7.02 (d, J = 16.3 Hz, 1H),

6.92 (dd, J = 5.6, 3.4 Hz, 2H), 6.89 (d, J = 13.9 Hz, 1H), 6.68 (d, J = 2.2 Hz, 2H), 6.47

– 6.39 (m, 1H), 6.08 (ddtd, J = 17.2, 10.5, 5.4, 3.4 Hz, 3H), 5.44 (ddq, J = 17.2, 3.3,

1.6 Hz, 3H), 5.31 (dq, J = 10.5, 1.5 Hz, 3H), 4.56 (dq, J = 5.3, 1.6 Hz, 6H). ^{13}C-NMR

(101 MHz, CDCl$_3$) δ (ppm): 160.01, 158.50, 139.76, 133.35, 133.27, 130.16, 128.82,

127.89, 126.69, 117.87, 117.82, 115.05, 105.46, 101.14, 69.00, 68.93. HRMS (ES+):

m/z: calcd for $C_{23}H_{24}O_3$ [M + H]$^+$: 349.18; found: 349.1738; calcd for $C_{23}H_{24}O_3$ [M + Na

+ H$_2$O]$^+$: 388.17; found: 388.1988.

Preparation of prepolymers and cured resins

According to the resin formula in Table 1, appropriate amounts of AER (or DBA)

and the corresponding amounts of BMI were added into the beakers. Then the

mixture was continuously stirred at 140 °C to completely melt, and when the liquid

was completely clear and transparent, the prepolymer of BMI/AER (or BMI/DBA) was

obtained. Next, the mixture was degassed under vacuum at 110 °C for 1 h, and then

poured into a preheated mold. After that, the mold was put into an oven for curing of

resins with the protocol of 150 °C/2 h + 180 °C/2 h + 200 °C/2 h + 220 °C/2 h + 240

°C/4 h. Finally, the cured resins were coded according to the molar ratio of allyl group

to maleimide functional group. For example, BA-0.8 represents that the molar ratio of

allyl group to maleimide functional group in BMI/AER is 1:0.8.

Characterizations

Fourier transform infrared (FT-IR) spectra were recorded between 650 and 4000

cm^{-1} with a resolution of 2 cm^{-1} on a Nicolet iS50 FT-IR spectrometer (Thermo Fisher

Scientific, USA). Nuclear magnetic resonance (NMR) spectra were recorded on a

Bruker Avance III HD 400 MHz (Germany) with $CDCl_3$ as the solvent. High resolution

mass spectra (HRMS) were characterized on a MALDI SYNAPT MS

ultra-performance liquid chromatography-tandem mass spectrometry (Waters, USA).

The curing behaviors of the resins were studied using a NETZSCH DSC 204 F1

(Germany) differential scanning calorimeter (DSC) ranging from 50 °C to 300 °C with

a heating rate of 10 °C min^{-1} under a nitrogen atmosphere. The Claisen

rearrangement of AER was also studied by DSC ranging from 50 °C to 280 °C with a

heating rate of 10 °C min^{-1} under a nitrogen atmosphere.

Thermogravimetric analyses (TGA) were performed on a TGA/1100SF

instrument (Mettler Toledo, Switzerland). Approximately 10 mg of samples was

heated from 50 °C to 800 °C with a temperature increment of 10 °C min^{-1}, under the

purified nitrogen flow rate of 50 mL min^{-1}. The dynamic mechanical analyses (DMA) were conducted using Q800 dynamic thermomechanical analyzer (TA Instruments, USA) at 1 Hz with the heating rate of 3 ℃ min^{-1} from 50 ℃ to 400 ℃. Each specimen was fixed to a double cantilever clip, and the dimension was 60 mm × 10 mm × 4 mm.

The impact strengths were tested according to GB/T-1843-2008 standard using a HIT-2492 Charpy impact machine tester (Chengde Jinjian Testing Instrument Co., Ltd, China). The flexural strengths were measured according to GB/T 9341-2008 standard using a 5967X electronic universal testing machine (ITW, USA) at a crosshead speed of 2 mm min^{-1}. The dimension of each specimen was 80 mm × 10 mm × 4 mm.

Microscale combustion calorimetry (MCC) tests were carried on a FAA-PCFC micro-scale combustion calorimeter (FTT, UK). 5 mg of a sample was heated from room temperature to 650 °C at a heating rate of 60 °C min^{-1}. The limiting oxygen index (LOI) test was performed using a 5801-A oxygen index apparatus (Suzhou Vouch Testing Technology Co., Ltd, China) with a magnetodynamic oxygen analyzer, according to the ASTM D2863-2017 standard. The dimension of each sample was 130 mm × 6.5 mm × 3 mm. The vertical burning (UL94) test was performed on a 5402-A instrument (Suzhou Vouch Testing Technology Co., Ltd, China) following ASTM D3801-2010 standard with the dimension of 130 mm × 13 mm × 3 mm.

Scanning electron microscope (SEM, Hitachi S-4800, Japan) was employed to observe the morphology of the samples after LOI test under the accelerating voltage

of 3.0 kV. All samples should be sprayed with gold to enhance the electric field signal

intensity before the test. An InVia Reflex laser confocal Raman spectroscope

(Renishaw, UK) with a 532 nm argon laser line was applied to study the degree of

graphitization of residue char of samples. Thermogravimetric analysis infrared

(TG-IR) spectra were recorded using a TL9000 thermogravimetry-infrared combined

instrument (PerkinElmer, USA). 10 ± 0.02 mg of samples was heated from 50 °C to

850 °C with a temperature increment of 20 °C min^{-1}, under the purified nitrogen flow

rate of 50 mL min^{-1}.

Results and discussion

Synthesis and characterization of AER

As shown in Scheme 1, the AER was synthesized by one-step nucleophilic

substitution reaction, which is a yellow viscous liquid (Figure S1a). It is easily soluble

in common organic solvents, such as chloroform, ethanol, acetone, and so on,

determined by dissolution test. The chemical structure of AER was characterized by

^{1}H-NMR and ^{13}C-NMR. In the ^{1}H-NMR spectrum (Figure 1a), the characteristic peaks

at 7.44 ppm (H_e), 6.92 ppm (H_d), 6.68 ppm (H_h) and 6.42 ppm (H_i) are attributed to the

protons on the two benzene rings of AER. Because of the strong conjugation with the

two benzene rings, the characteristic peaks of the double bond are found to move to

7.02 ppm (H_g) and 6.89 ppm (H_f). In addition, the characteristic peaks attributed to

allyl protons are observed at 6.08 ppm (H_b), 5.44 ppm and 5.31 ppm (H_a), and 4.56

ppm (H_c). In ^{13}C-NMR spectrum (Figure 1b), the characteristic peaks at 160.0 ppm

(C_l, 2C) and 158.5 ppm (C_d, 1C) represent the C atoms directly connected to the O atom on the benzene ring. The characteristic peaks at 139.8 ppm (C_j, 1C), 130.2 ppm (C_g, 1C), 127.9 ppm (C_f, 2C), 115.1 ppm (C_e, 2C), 105.5 ppm (C_k, 2C), and 101.1 ppm (C_m, 1C) are attributed to other carbon atoms on the benzene ring. The characteristic peaks at 128.8 ppm (C_i, 1C) and 126.7 ppm (C_h, 1C) are assigned to the carbon atoms on the double bond connecting the two benzene rings. In addition, the characteristic peaks belonging to allyl carbon atoms are observed at 135.3 ppm (C_b and $C_{b'}$, 3C), 117.8 ppm (C_a and $C_{a'}$, 3C) and 69.0 ppm (C_c and $C_{c'}$, 3C).
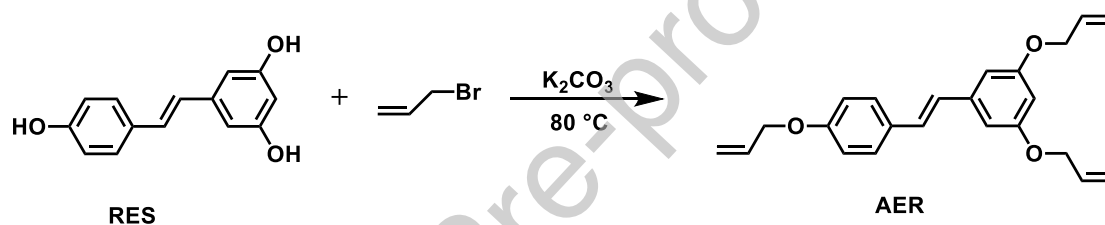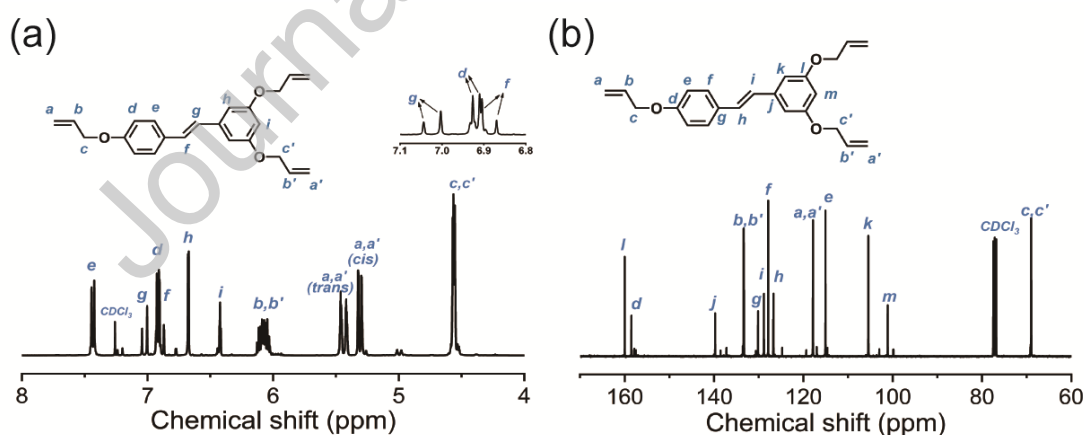

Scheme 1. Synthesis of AER.

Figure 1. (a) ^{1}H-NMR and (b) ^{13}C-NMR spectra of AER.

The FT-IR spectra of RES and AER were collected, as shown in Figure S1b. After reaction, the disappearance of the characteristic absorption peak (3196 cm^{-1}) of

phenol hydroxyl on RES is observed, as well as the appearance of the characteristic

absorption peaks of methylene (2964 cm^{-1}) and ether bond (1248 cm^{-1}). The mass

spectrum also demonstrates the expected structure of AER (Figure S1c). In addition,

in the non-isothermal DSC curves of Figure S1d, an obvious exothermic peak is found

for AER at 207-270 °C, while no exothermic peak is found for DBA. It is due to the

Claisen rearrangement of allyl aromatic ether structure in AER at high temperature,

resulting in the formation of allyl phenyl structure. But DBA itself is an allyl phenyl

compound, so similar rearrangement reaction will not occur.[32, 33] These above

characterization results fully confirmed the successful synthesis of AER.

Curing behaviors and mechanism of BA resins

In order to study the curing behavior of BA resins, non-isothermal DSC test was

carried out. Figure 2 depicts the DSC curves of BD and BA prepolymers. Each curve

shows a single curing exothermic peak, and the exothermic peaks of the BA

prepolymers appear at lower temperatures (243.3 °C-246.1 °C) compared with that of

BD prepolymers (255.0 °C-270.3 °C). It is reported that resveratrol-based

benzoxazine resin also displayed a reduced curing temperature, but it was not

explained.[27] In this case, it may be attributed to the Claisen rearrangement reaction

of allyl aromatic ether structure in AER, the non-isothermal DSC exothermic peak of

which appears at approximatively 241 °C (Figure S1d). Moreover, compared to DBA,

AER has more reactive functional groups and higher curing reactivity, which may also

lead to a lower curing temperature of BA prepolymers. Therefore, the curing

procedure of BA resins can follow the typical curing procedure of BD resins (150 °C/2

h + 180 °C/2 h + 200 °C/2 h + 220 °C/2 h + 240 °C/4 h), to ensure a complete curing.

By comparing the FT-IR spectra before and after curing of the resin (Figure S2), it can

be found that the characteristic absorption peak of the maleimide ring at 713 cm^{-1} has

completely disappeared, indicating that the resins have been cured completely. DSC

was further employed to verify whether BD and BA resins can be fully cured at the

typical curing procedure. As shown in Figure S3, there is no obvious exothermic peak

both for the cured BD and BA resins, indicating that the resins have been completely
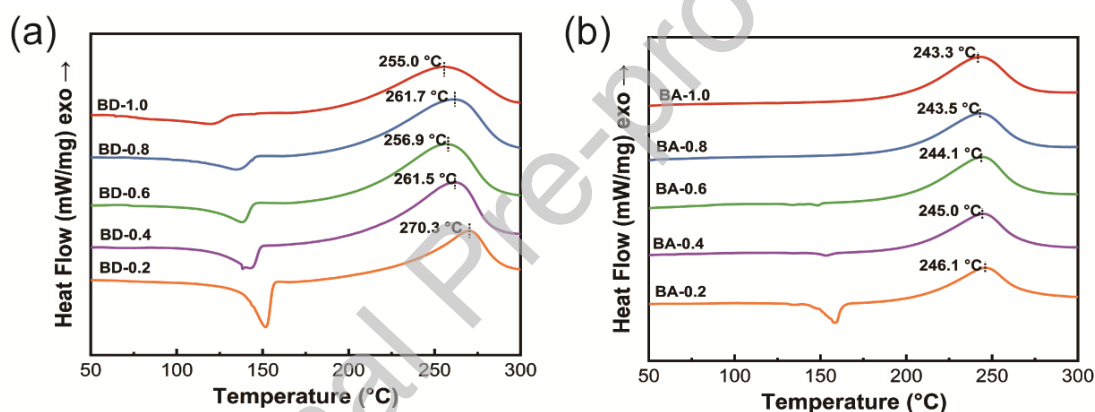
cured following the above curing procedure.

Figure 2. DSC curves of (a) BD and (b) BA prepolymers.

In order to clearly evaluate the chemical reaction in curing process, the FT-IR

spectra (Figure 3) of BD-0.8 and BA-0.8 resins at different curing stages were

recorded, and the corresponding digital photos of BD-0.8 and BA-0.8 resin at different

curing stages are shown in the Figure S4. In the spectra of BD-0.8 resin, as the curing

progresses, both the characteristic absorption peaks of allyl groups (1637 cm^{-1} and

912 cm^{-1}) and maleimide ring (1607 cm^{-1} and 712 cm^{-1}) gradually weaken.

Furthermore, the characteristic peak of allyl groups becomes weak rapidly, indicating

that the ene reaction takes place at the early stage of curing. However, the absorption

peaks of maleimide ring exist over 200 °C, indicating that the self-polymerization of

maleimide occurs at a high temperature, generally higher than 200 °C.[17] But for

BA-0.8 resin, besides the above similar curing mechanism, it is found that the C=C

bond of AER (950 cm^{-1}) still exists after curing. It may be that the C=C bond of the

stilbene structure in AER cannot participate in the curing reaction effectively, because

of steric hindrance. The retention of stilbene structure after curing at high temperature

is also reported in studies on other resveratrol-based thermosetting resins.[26, 28, 34]

Moreover, the absorption peak of phenolic hydroxyl group (3466 cm^{-1}) is observed in

the FT-IR spectrum of BA-0.8 resin after complete curing (Figure S2b), which proves

that Claisen rearrangement occurs during the curing process of BA resins. In

conclusion, the possible chemical reactions during the curing process of BD and BA

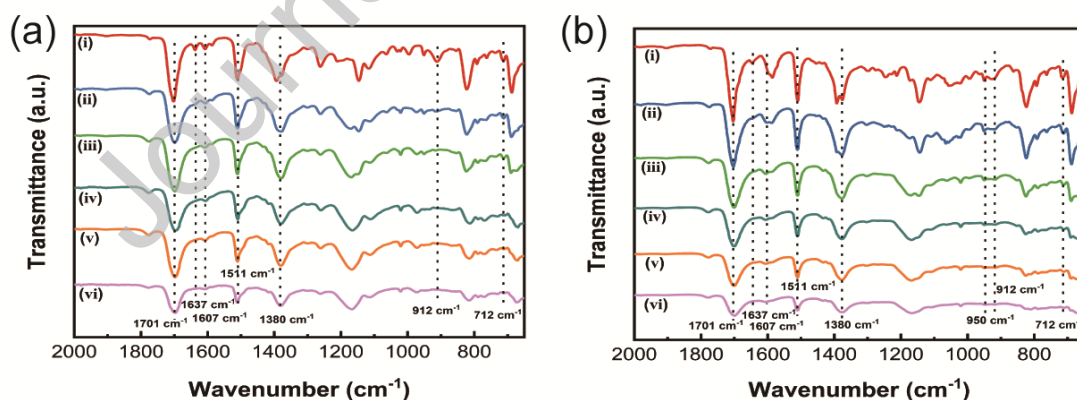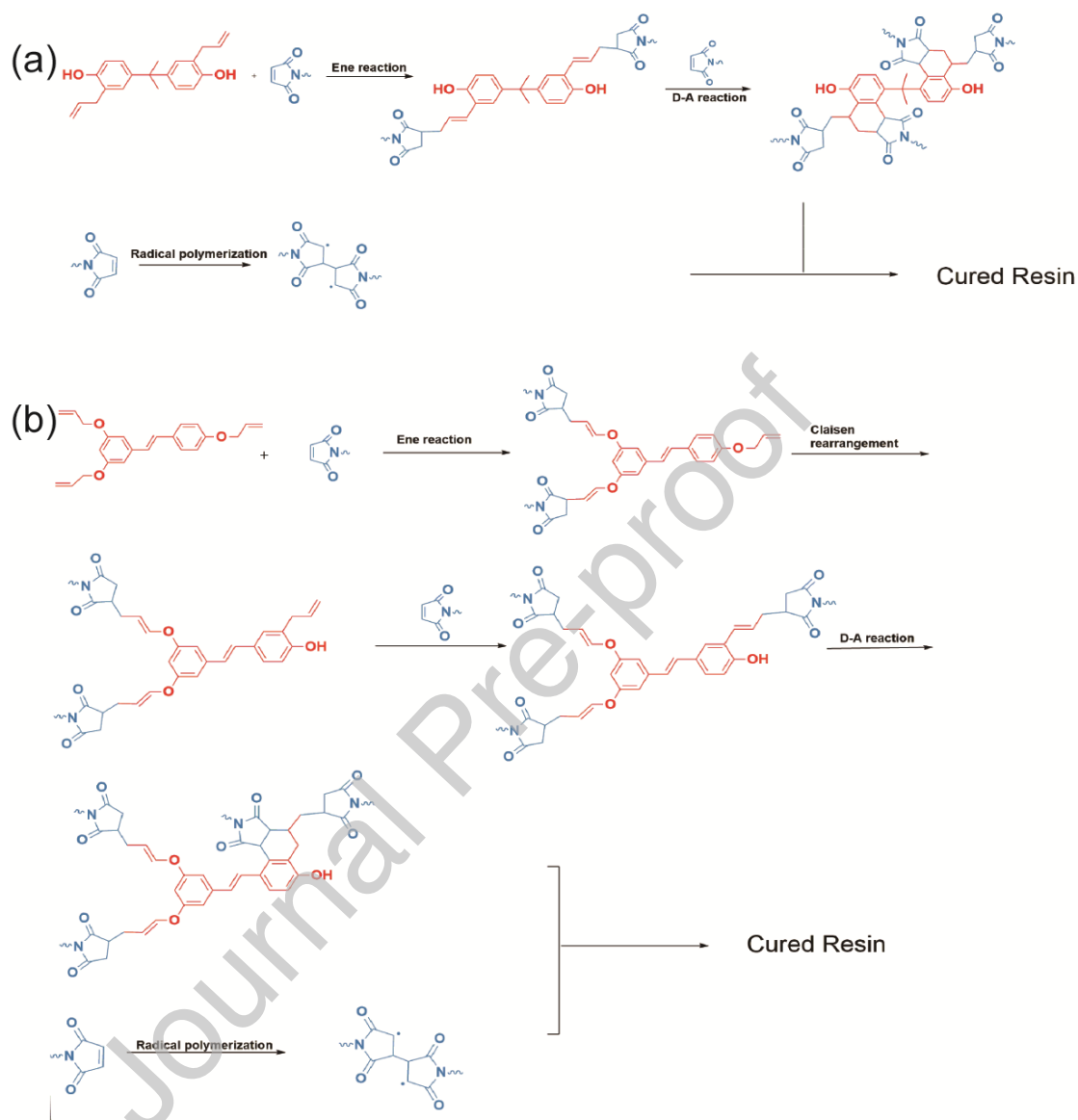resins are shown in the Scheme 2.

Figure 3. FT-IR spectra of (a) BD-0.8 and (b) BA-0.8 resins at different curing stages:

(i) prepolymer, (ii) 150 °C/2 h, (iii) 150 °C/2 h + 180 °C/2 h, (iv) 150 °C/2 h + 180 °C/2

h + 200 °C/2 h, (v) 150 °C/2 h + 180 °C/2 h + 200 °C/2 h + 220 °C/2 h, (vi) 150 °C/2 h

+ 180 °C/2 h + 200 °C/2 h + 220 °C/2 h + 240 °C/4 h.

Scheme 2. Curing reactions of (a) BD and (b) BA resins.

Thermal properties of cured BA resins

For thermosetting resins, T_g is one of the most important parameters, which

determines the service temperature of materials.[35] The T_g of a thermosetting resin

is usually taken as the maximum peak temperature on the loss tangent curve in the

DMA test.[36] Figure 4 shows the DMA curves of cured BD and BA resins, and Table 2 gives the obtained T_g values. With the increase of the amount of allyl group, the T_g gradually decreases, which is due to the chain extension by allyl group reducing the crosslinking density of cured resin. Even so, the T_g of cured BA resin is higher than that of cured BD resin. In particular, the T_g of BA-0.6, BA-0.4 and BA-0.2 tend to be higher than 400 °C, even higher than the thermal decomposition temperature. For cured BA-0.8 resin, the T_g is still as high as 388 °C, which is about 54 °C higher than that of cured BD-0.8 resin. Moreover, the storage modulus at glassy state of cured BA resins is also observed to be higher than that of cured BD resins. This is due to the special structure of AER with tri-functionality and stiffness conjugated stilbene backbone, giving the cured products higher crosslinking density and chain rigidity compared with that of DBA. Because the T_g of thermosetting resin usually represents the highest end-use temperature of materials, so DMA results demonstrate that the cured BA resin has excellent heat resistance.
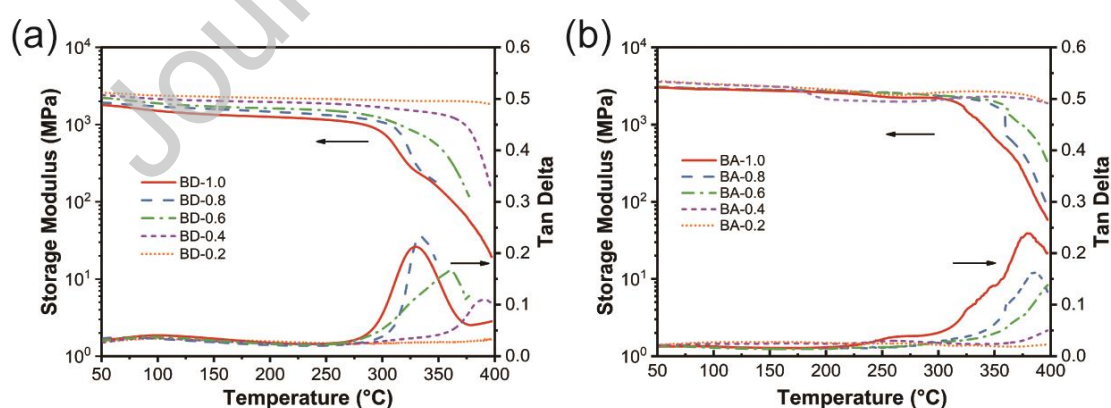

Figure 4. DMA curves of cured BD (a) and BA (b) resins.

Study of thermal degradation behavior of thermosetting resin is also important, which decides the thermal stability of materials.[35, 37] TGA was used to test the thermal weight loss of the cured BD and BA resins. The thermal decomposition temperature of 5% weight loss is defined as the onset of decomposition temperature ($T_{d5\%}$), and the peak temperature in DTG curve is defined as the temperature of maximum weight loss rate (T_{max}). Figure 5 and Table 2 show that, whether it is BD or BA resin, as the amount of modifier increases, the thermal stability of cured resin decreases, and the $T_{d5\%}$, T_{max} and char yield at 800 °C ($Y_{800\,°C}$) of the cured resins all exhibit a decline. This is because whether DBA or AER, its thermal stability is far inferior to the BMI resin itself, so when DBA or AER is added to the resin system, it will be thermally decomposed at first. Furthermore, it is found that although the cured BA and BD resins with the same molar ratio of imide to allyl groups have similar $T_{d5\%}$ and T_{max}, the $Y_{800\,°C}$ of cured BA resins are much higher than that of cured BD resins. For example, compared with BD-1.0 resin, BA-1.0 resin shows a significant increase of the $Y_{800\,°C}$ of cured product from 30.2 to 48.4 wt%. The increase of $Y_{800\,°C}$ may be related to the structure of AER. The stilbene backbone makes AER molecule form a large conjugated structure, which is stable and difficult to be destroyed, and will be converted into the residue char at high temperature.[38]
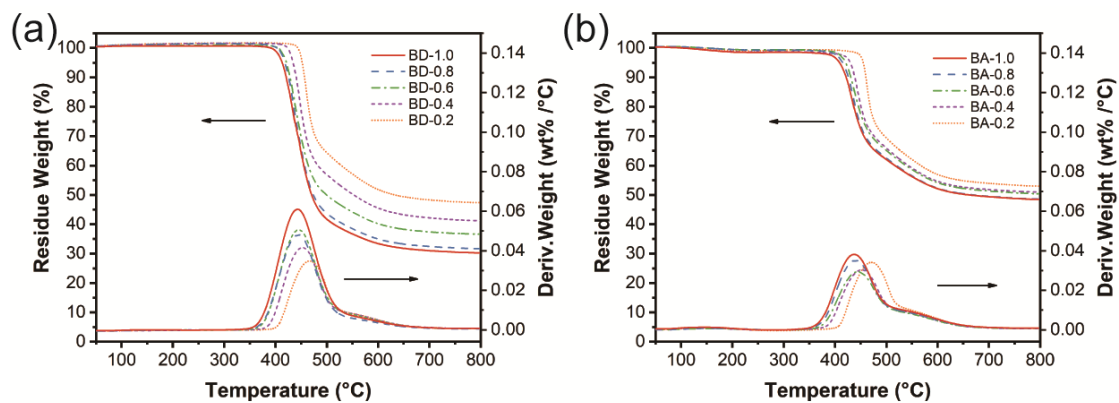
Figure 5. TGA and DTG curves of cured BD (a) and BA (b) resins.

Table 2. Typical parameters of cured BD and BA resins from the DMA and TGA tests.

Resin Code	T_g	[a]Storage Modulus	$T_{d5\%}$	T_{max}	$Y_{800\,°C}$
	(°C)	(MPa)	(°C)	(°C)	(wt%)
BD-0.2	-	2592.7	452.0	466.5	47.3
BD-0.4	-	2414.5	434.3	452.5	41.2
BD-0.6	347.0	2224.0	421.2	445.2	36.6
BD-0.8	334.3	1932.7	418.3	444.3	31.7
BD-1.0	324.5	1801.1	413.2	443.0	30.2
BA-0.2	-	3659.4	455.2	471.2	52.9
BA-0.4	-	3578.6	430.2	452.0	51.0

BA-0.6	-	3110.0	421.0	444.7	50.3
BA-0.8	388.0	3101.6	415.0	440.0	48.6
BA-1.0	378.7	3035.3	409.0	437.5	48.4

aThe storage modulus of cured resins at 50 °C

Mechanical properties of cured BA resins

The mechanical properties of cured BA resins were investigated by bending and impact tests, and compared with that of cured BD resins. Figure 6 shows the test results of flexural modulus and flexural strength. With the increase of allyl compound content in both BD and BA resins, the flexural modulus of the cured resin decreases gradually while the flexural strength increases. When the molar ratio of maleimide to allyl groups is 1:0.8, the flexural strength of the cured resins reaches the maximum. This is because, compared to unmodified BMI resin, the chain extension by allyl group reduces the crosslinking density of cured resin, and thus increases the toughness of the material. The impact test results also demonstrate the toughening effect of the allyl compound modified BMI resins (Figure S5). However, the cured BA resins show a higher flexural modulus and lower flexural strength and impact strength than the cured BD resins, indicating that the cured BA resins are less ductile than the cured BD resins. This is because AER with the tri-functionality and stiffness conjugated stilbene backbone gives the cured products higher crosslinking density and chain rigidity compared with DBA. Even so, the toughness of the cured BA resins is still superior to that of the unmodified BMI resin.
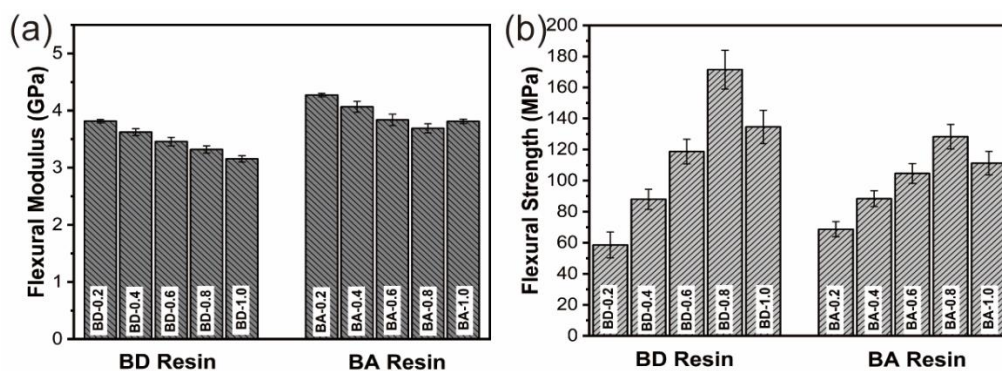
Figure 6. Flexural modulus (a) and flexural strength (b) of cured BD and BA resins.

Flame retardancy and mechanism of cured BA resins

Above results of TGA test show that the char yield of cured BA resins is significantly improved, so it is speculated that the cured BA resins has excellent flame retardancy properties.[16] In order to evaluate the flame retardancy of BA resins, the cured BA-0.8 resin with optimal comprehensive properties was selected for a series of flame retardant tests, and the cured BD-0.8 resin was used as the contrast one. As is well-known, the LOI and UL-94 tests are effective methods to evaluate the flame retardancy of materials. The LOI values and UL-94 test results are given in Table 3. The LOI value of cured BA-0.8 resin reaches 37.7%, which is much higher than that of cured BD-0.8 resin (27.1%). During the UL-94 test, even though neither the cured BD-0.8 resin nor BA-0.8 resin was dripping, the cured BA-0.8 resin exhibited an improved UL94 level from V-1 to V-0 compared with the cured BD-0.8 resin. For the cured BA-0.8 resin, a shorter burning time (t_1/t_2) was presented. A similar phenomenon was also observed in the fire test (see Video S1, S2 and Figure S6).

Table 3. LOI values and UL-94 test results of cured BD-0.8 and BA-0.8 resins.

Resin	LOI (%)	Flammability from vertical burning testing		
		UL-94 level	Dripping	$^a t_1/t_2$ (s)
BD-0.8	27.1	V-1	None	11.2/26.3
BA-0.8	37.7	V-0	None	1.0/2.9

^{a}After-flame time of the first and second flame tests.

MCC is a useful technique to study the relationship between chemical structure and combustion behavior of polymers based on oxygen consumption theory.[39] In MCC tests, many characteristic parameters can be obtained, including the heat release rate (HRR), temperature of peak heat release rate (TPHRR), total heat release (THR), and heat releasing capacity (HRC). The HRR-temperature curves and THR-temperature curves of cured BD-0.8 and BA-0.8 resins are shown in Figure 7a and b, respectively. The corresponding parameters obtained from MCC test are given in Table 4. Figure 7a shows that a high and wide peak appears in the HRR-temperature curve of cured BD-0.8 resin, while the cured BA-0.8 resin exhibits a much weaker and narrower peak. In addition, the cured BA-0.8 resin also has a higher TPHRR, which reaches up to 471 °C. The THR-temperature curves in Figure 7b further reveal that the THR of cured BA-0.8 resin is only 7.5 kJ g^{-1}, which is much lower than that of cured BD-0.8 resin (22.5 kJ g^{-1}). It indicates a superior effect of AER compared with DBA in inhibition of the heat release rate and heat release of cured resins during MCC test. Moreover, the HRC of cured BA-0.8 resin is calculated as 122.5 J g^{-1} K^{-1}, which is only 29.5% of the value for cured BD-0.8 resin. In earlier

studies Lyon et al. proposed an empirical relationship of HRC values with the results of UL-94 and LOI tests for polymers that thermally decompose in single-step. They observed that HRC= 100–200 J g^{-1} K^{-1} corresponds to self-extinguishing in UL 94 test (V-0/5V) and LOI = 30–40.[40] Our test results for the cured BA-0.8 resin are in good agreement with this empirical regime.
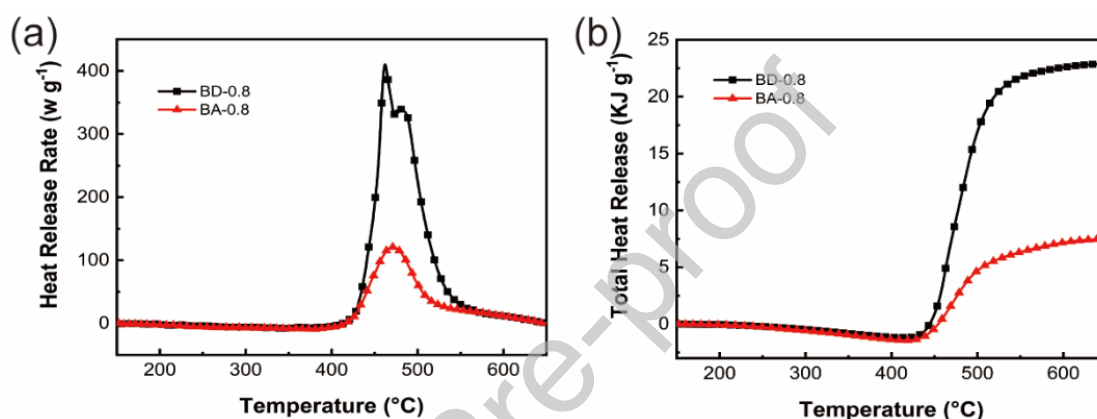

Figure 7. (a) Heat release rate-temperature and (b) total heat release curves from MCC tests for cured BD-0.8 and BA-0.8 resins.

Table 4. Parameters obtained from MCC test for the cured BD-0.8 and BA-0.8 resins.

Samples	TPHRR (°C)	THR (kJ g^{-1})	HRC (J g^{-1} K^{-1})
BD-0.8	462.0	22.5	415.7
BA-0.8	471.1	7.5	122.5

It is found that the LOI values measured in this study fit well to the equation proposed by van Krevelen:[41]

$$LOI = 17.5 + 0.4\ CR$$

(1)

where CR is the char yield (%) obtained from TGA under nitrogen. It indicates that the excellent charring of cured BA-0.8 resin is beneficial for good flame retardancy. We further investigated the morphology and structure of the char formed after burning test, as well as the generated volatiles during the thermal degradation process, to better understand the flame-retardant mechanism.

The morphology of residue chars on the surface of the samples after the LOI test was characterized by SEM (Figure 8a, b, d, and e). The char structures of cured BD-0.8 resin and BA-0.8 resin are similar. Both structures are easy penetrable considering the size of pores being much larger than the size of gas molecules. The heat insulation for the two cases may be also very similar. In addition, the obtained residue char was tested by Raman spectroscopy, and the graphitization degree of carbonaceous layer was evaluated. The obtained Raman spectra are shown in the Figure 8c and f. Only two typical absorptions appear for the residue char of both cured BD-0.8 and BA-0.8 resins. The D peak at 1350 cm^{-1} belongs to the disordered vibration peak of graphite carbon, and the G peak at 1580 cm^{-1} belongs to the in-plane vibration peak of sp^2 carbon atom. I_D and I_G represent the integral area of D peak and G peak, respectively. Noted that the lower the I_D/I_G value, the higher the graphitization degree of the residue char.[42, 43] From the calculation results, the char of cured BA-0.8 resin has a much lower I_D/I_G value (0.60) than that of cured BD-0.8 resin

(1.32), indicating its higher degree of graphitization. The char with higher

graphitization degree is considered to bring more stable carbonaceous char.[44]

Thus, the superior flame retardancy of cured BA-0.8 resin to that of cured BD-0.8

resin is mainly due to the increased and more stable residue char, which may be

attributed to the stilbene structure in AER promoting graphitization and char

formation. However, because of its porous morphology, the char cannot play a role in

blocking oxygen or preventing the escape of organic volatiles during the combustion
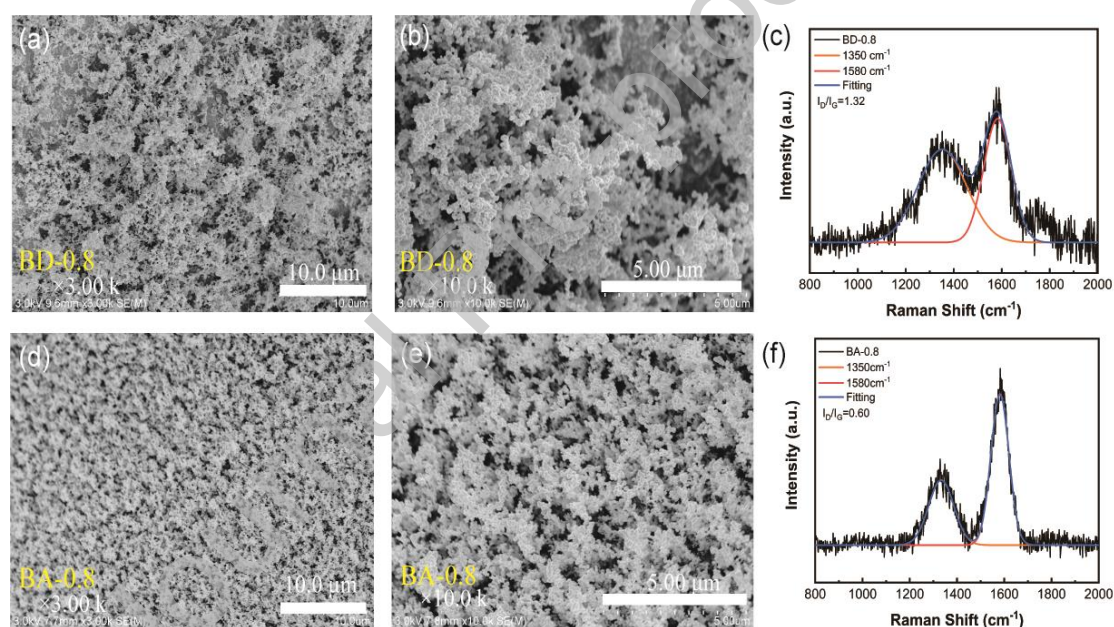
process.

Figure 8. SEM images and Raman spectra of the residue char of cured BD-0.8 resin

(a-c) and BA-0.8 resin (d-f).

Figure S7 shows the TGA and DTG curves of cured BD-0.8 and BA-0.8 resins

from TG-IR tests. Although the onset of decomposition temperature of cured BA-0.8

resin is slightly lower than that of cured BD-0.8 resin, the char yield of cured BA-0.8

resin at 850 °C is 53.1%, which is about 26.3% higher than that of cured BD-0.8 resin

(26.8%). Moreover, the thermal decomposition rate of cured BA-0.8 resin is much lower than that of cured BD-0.8 resin revealed in DTG curves. The higher char yield of cured BA-0.8 resin indicates that cured BA-0.8 resin releases less fuel and other volatiles during thermal decomposition compared with cured BD-0.8 resin.

The chemical composition of gas pyrolysis products of cured BD-0.8 and BA-0.8 resins were investigated by TG-IR tests. Figure 9a and b show the FT-IR spectra of the volatiles of cured BD-0.8 and BA-0.8 resins at typical temperatures. For cured BD-0.8 resin, the characteristic peaks of CO_2 (2363, 2330 and 668 cm^{-1}) are observed at 384 °C, indicating the beginning of pyrolysis. When the temperature reaches the $T_{d5\%}$ (442 °C) of cured BD-0.8 resin, the characteristic peaks of CO_2 become stronger. Meanwhile, the characteristic peaks of other decomposition products begin to appear, including the peaks at 3650, 1374, 1616, 1507 and 1176 cm^{-1} attributed to H_2O, aromatic compounds, NO_2, nitrogen oxides and organonitrogen compounds, respectively. When the temperature reaches T_{max} (492 °C), the characteristic peaks of volatiles become the strongest, and the volatilization of flammable gases such as hydrocarbons (3017 and 2971 cm^{-1}) and carbonyl compounds (1717 cm^{-1}) are also found. Similar volatiles are also found in the FT-IR spectra of cured BA-0.8 resin (Figure 9b). However, by combining the results of three-dimensional FT-IR (Figure 9c and d) with the curves of absorbance of pyrolysis products versus temperature (Figure S8), it can be found that the release of combustible gases (hydrocarbons, aromatic compounds and organonitrogen compounds) is greatly reduced.

The effective heat of combustion of the volatiles (h_c^0) can be calculated as follows:[39]

$$h_c^0 = \frac{THR}{1-\mu} \qquad (2)$$

where *THR* is the total heat release obtained by MCC, and μ is the char yield (%) obtained from TGA. For cured BA-0.8 resin, its h_c^0 value is about 14.6 kJ g^{-1}, which is only 44.3% of cured BD-0.8 resin. The calculated h_c^0 value further supports the conclusion that fewer combustible volatiles are produced by the thermal decomposition of cured BA-0.8 resin per unit mass. The decrease of combustible volatile emissions indicates less fuel supply to the flame during combustion.
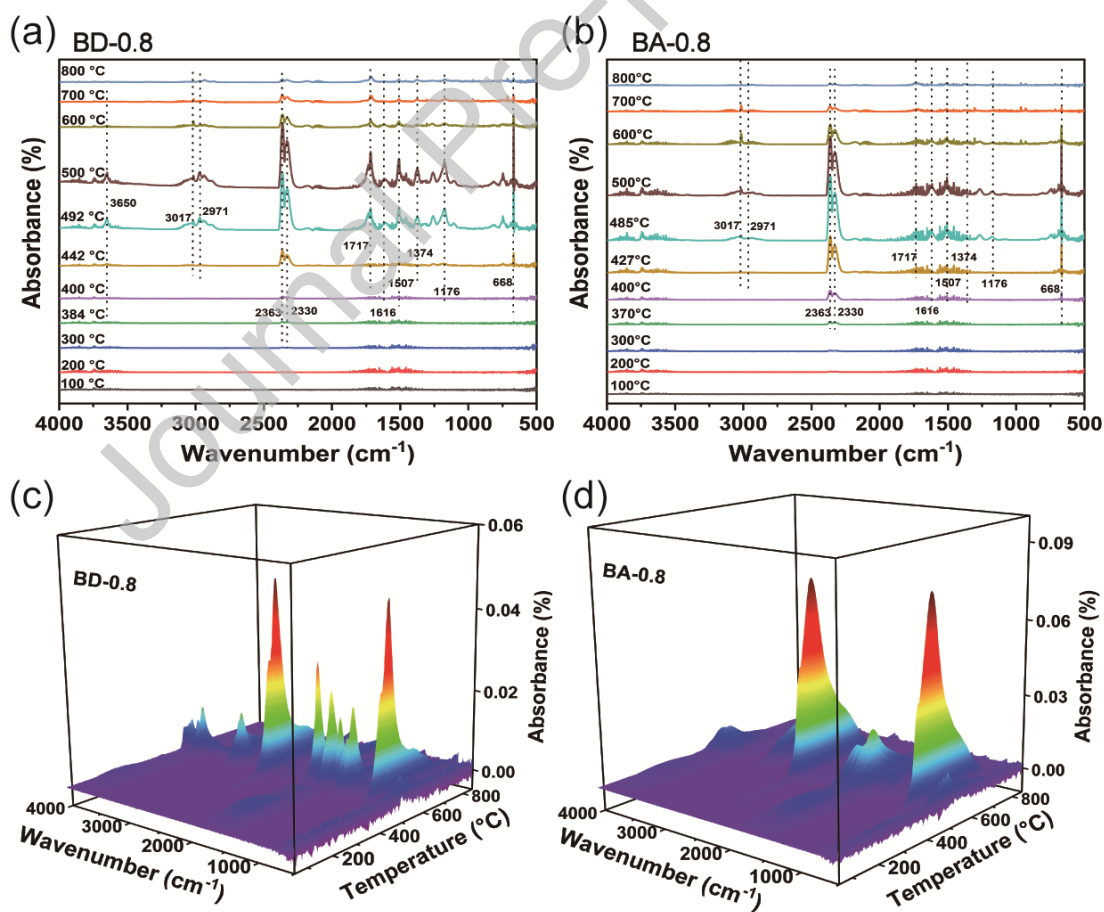
Figure 9. FTIR spectra of pyrolysis products of cured BD-0.8 (a) and BA-0.8 (b) resins at typical temperatures; three-dimensional TG-IR spectra of pyrolysis products of cured BD-0.8 (c) and BA-0.8 (d) resins.

Based on above discussion, the good flame retardancy of cured BA resin is mainly attributed to the excellent charring and decrease of combustible volatiles.

Conclusion

A bio-based allyl compound AER was successfully synthesized by using resveratrol and allyl bromide in a one-step process. Then a series of BA resins were obtained by blending bismaleimide resin with different contents of AER. Compared with traditional petroleum-based BD resins, BA resins had a lower polymerization temperature, which is advantageous for processing. Among the cured resins, BA-0.8 resin had an excellent comprehensive performance, with T_g, $T_{d5\%}$ and $Y_{800\,°C}$ of 388 °C, 415 °C and 48.6%, respectively, as well as a superior toughness to the unmodified BMI resin. In addition, due to the special structure of AER, the cured BA-0.8 resin also showed excellent flame retardancy, including low heat release capacity and total heat release. LOI, UL-94 and TGA results indicated that the cured BA-0.8 resin possessed excellent flame retardancy (V-0 level, LOI = 37.7% and $Y_{800\,°C}$ = 48.6%). The good flame retardancy of cured BA-0.8 resin was mainly attributed to the excellent charring and decrease of combustible volatiles. This research provides a new method for preparing high-performance and flame-retardant materials from

natural renewable resources, showing the great potential of green resources in cutting-edge applications.

Acknowledgements

References

[1] R.J. Iredale, C. Ward, I. Hamerton, Modern advances in bismaleimide resin technology: A 21st century perspective on the chemistry of addition polyimides, Prog. Polym. Sci. 69 (2017) 1-21.

[2] H. Stenzenberger, Recent advances in thermosetting polyimides, Br. Polym. J. 20(5) (1988) 383-396.

[3] Z.y. Yerlikaya, Z. Öktem, E. Bayramli, Chain-Extended bismaleimides. I. Preparation and characterization of maleimide-terminated resins, J. Appl. Polym. Sci. 59(1) (1996) 165-171.

[4] M. Satheesh Chandran, C.P. Reghunadhan Nair, 12 - Maleimide-Based Alder-Enes, in: H. Dodiuk, S.H. Goodman (Eds.), Handbook of Thermoset Plastics (Third Edition), William Andrew Publishing, Boston, 2014, pp. 459-510.

[5] D. Zhuo, A. Gu, G. Liang, J.-t. Hu, L. Yuan, X. Chen, Flame retardancy materials based on a novel fully end-capped hyperbranched polysiloxane and bismaleimide/diallylbisphenol A resin with simultaneously improved integrated performance, J. Mater. Chem. 21(18) (2011) 6584-6594.

[6] G. Liang, A. Gu, Toughening Bismaleimide Resins by N-Allyl Aromatic Amine, Polym. J. 29(7) (1997) 553-556.

[7] Z. Wang, W. Wu, M.H. Wagner, L. Zhang, S. Bard, Synthesis of DV-GO and its effect on the fire safety and thermal stability of bismaleimide, Polym. Degrad. Stab. 128 (2016) 209-216.

[8] N. Li, Y. Li, X. Hao, J. Gao, A comparative experiment for the analysis of microwave and thermal process induced strains of carbon fiber/bismaleimide composite materials, Compos. Sci. Technol. 106 (2015) 15-19.

[9] Q. Yu, P. Chen, Y. Gao, K. Ma, C. Lu, X. Xiong, Effects of electron irradiation in space environment on thermal and mechanical properties of carbon fiber/bismaleimide composite, Nucl. Instrum. Methods Phys. Res., Sect. B 336 (2014) 158-162.

[10] H. Tang, N. Song, Z. Gao, X. Chen, X. Fan, Q. Xiang, Q. Zhou, Preparation and properties of high performance bismaleimide resins based on 1,3,4-oxadiazole-containing monomers, Eur. Polym. J. 43(4) (2007) 1313-1321.

[11] X. Zeng, S. Yu, R. Sun, J.-b. Xu, Mechanical reinforcement while remaining electrical insulation of glass fibre/polymer composites using core–shell CNT@SiO$_2$ hybrids as fillers, Composites, Part A 73 (2015) 260-268.

[12] Z.-Y. Wang, J.-C. Ho, W.-J. Shu, Studies of fluorine-containing bismaleimide resins part I: Synthesis and characteristics of model compounds, J. Appl. Polym. Sci. 123(5) (2012) 2977-2984.

[13] Y. Jiao, L. Yuan, G. Liang, A. Gu, Facile Preparation and Origin of High-k Carbon Nanotube/Poly(Ether Imide)/Bismaleimide Composites through Controlling the Location and Distribution of Carbon Nanotubes, J. Phys. Chem. C 118(41) (2014) 24091-24101.

[14] Y. Zhang, J. Lv, Y. Liu, Preparation and characterization of a novel fluoride-containing bismaleimide with good processability, Polym. Degrad. Stab. 97(4) (2012) 626-631.

[15] Z. Ren, Y. Cheng, Y. Li, F. Xiao, Preparation and characterization of soluble bismaleimide-triazine resins based on asymmetric bismaleimide, J. Appl. Polym. Sci. 134(9) (2017) 44519.

[16] J.-T. Miao, L. Yuan, G. Liang, A. Gu, Biobased bismaleimide resins with high renewable carbon content, heat resistance and flame retardancy via a multi-functional phosphate from clove oil, Mater. Chem. Front. 3(1) (2019) 78-85.

[17] J. Mijović, S. Andjelić, Study of the Mechanism and Rate of Bismaleimide Cure by Remote in-Situ Real Time Fiber Optic Near-Infrared Spectroscopy, Macromolecules 29(1) (1996) 239-246.

[18] S. Zahir, M.A. Chaudhari, J. King, Novel high temperature resins based on bis(4-maleimido-phenyl)methane, Makromol. Chem., Macromol. Symp. 25(1) (1989) 141-154.

[19] M.V. Maffini, B.S. Rubin, C. Sonnenschein, A.M. Soto, Endocrine disruptors and reproductive health: The case of bisphenol-A, Mol. Cell. Endocrinol. 254-255 (2006) 179-186.

[20] X. Chen, A. Gu, G. Liang, L. Yuan, D. Zhuo, J.-t. Hu, Novel low phosphorus-content bismaleimide resin system with outstanding flame retardancy and low dielectric loss, Polym. Degrad. Stab. 97(5) (2012) 698-706.

[21] M. Zwingelstein, M. Draye, J.-L. Besombes, C. Piot, G. Chatel, trans-Resveratrol and trans-ε-Viniferin in Grape Canes and Stocks Originating from Savoie Mont Blanc Vineyard Region: Pre-extraction Parameters for Improved Recovery, ACS Sustainable Chem. Eng. 7(9) (2019) 8310-8316.

[22] L. Chen, Y. Han, F. Yang, T. Zhang, High-speed counter-current chromatography separation and purification of resveratrol and piceid from Polygonum cuspidatum, J. Chromatogr. A 907(1) (2001) 343-346.

[23] J.M. Sales, A.V.A. Resurreccion, Maximising resveratrol and piceid contents in UV and ultrasound treated peanuts, Food Chem. 117(4) (2009) 674-680.

[24] C.K. Singh, X. Liu, N. Ahmad, Resveratrol, in its natural combination in whole grape, for health promotion and disease management, Ann. N. Y. Acad. Sci. 1348(1) (2015) 150-160.

[25] J.J. Cash, M.C. Davis, M.D. Ford, T.J. Groshens, A.J. Guenthner, B.G. Harvey, K.R. Lamison, J.M. Mabry, H.A. Meylemans, J.T. Reams, C.M. Sahagun, High T_g thermosetting resins from resveratrol, Polym. Chem. 4(13) (2013) 3859-3865.

[26] K. Zhang, M. Han, L. Han, H. Ishida, Resveratrol-based tri-functional benzoxazines: Synthesis, characterization, polymerization, and thermal and flame retardant properties, Eur. Polym. J. 116 (2019) 526-533.

[27] K. Zhang, M. Han, Y. Liu, P. Froimowicz, Design and Synthesis of Bio-Based High-Performance Trioxazine Benzoxazine Resin via Natural Renewable Resources, ACS Sustainable Chem. Eng. 7(10) (2019) 9399-9407.

[28] Y. Tian, Q. Wang, L. Shen, Z. Cui, L. Kou, J. Cheng, J. Zhang, A renewable resveratrol-based epoxy resin with high T_g, excellent mechanical properties and low flammability, Chem. Eng. J. 383 (2020) 123124.

[29] J. Hou, X. Chen, J. Sun, Q. Fang, A facile conversion of a bio-based resveratrol to the high-performance polymer with high T_g and high char yield, Polymer 200 (2020) 122570.

[30] L. Fang, Y. Tao, C. Wang, M. Dai, G. Huang, J. Sun, Q. Fang, Resveratrol-Based Fluorinated Materials with High Thermostability and Good Dielectric Properties at High Frequency, ACS Sustainable Chem. Eng. 8(45) (2020) 16905-16911.

[31] G. Huang, L. Fang, C. Wang, M. Dai, J. Sun, Q. Fang, A bio-based low dielectric material at a high frequency derived from resveratrol, Polym. Chem. 12(3) (2021) 402-407.

[32] A.M. Martín Castro, Claisen Rearrangement over the Past Nine Decades, Chem. Rev. 104(6) (2004) 2939-3002.

[33] M. Ge, J.-T. Miao, L. Yuan, Q. Guan, G. Liang, A. Gu, Building and origin of bio-based bismaleimide resins with good processability, high thermal, and mechanical properties, J. Appl. Polym. Sci. 135(10) (2018) 45947.

[34] Y. Tian, Q. Wang, K. Wang, M. Ke, Y. Hu, L. Shen, Q. Geng, J. Cheng, J. Zhang, From biomass resources to functional materials: A fluorescent thermosetting material based on resveratrol via thiol-ene click chemistry, Eur. Polym. J. 123 (2020) 109416.

[35] X. Zhang, R. Akram, S. Zhang, H. Ma, Z. Wu, D. Wu, Hexa(eugenol)cyclotriphosphazene modified bismaleimide resins with unique thermal stability and flame retardancy, React. Funct. Polym. 113 (2017) 77-84.

[36] Y. Wang, L. Yuan, G. Liang, A. Gu, Achieving ultrahigh glass transition temperature, halogen-free and phosphorus-free intrinsic flame retardancy for

bismaleimide resin through building network with diallyloxydiphenyldisulfide, Polymer 203 (2020) 122769.

[37] X. Zhou, S. Qiu, J. Liu, M. Zhou, W. Cai, J. Wang, F. Chu, W. Xing, L. Song, Y. Hu, Construction of porous g-C$_3$N$_4$@PPZ tubes for high performance BMI resin with enhanced fire safety and toughness, Chem. Eng. J. 401 (2020) 126094.

[38] L. Shang, X. Zhang, M. Zhang, L. Jin, L. Liu, L. Xiao, M. Li, Y. Ao, A highly active bio-based epoxy resin with multi-functional group: synthesis, characterization, curing and properties, J. Mater. Sci. 53(7) (2017) 5402-5417.

[39] B. Schartel, K.H. Pawlowski, R.E. Lyon, Pyrolysis combustion flow calorimeter: A tool to assess flame retarded PC/ABS materials?, Thermochim. Acta 462(1) (2007) 1-14.

[40] R.E. Lyon, R.N.Walters, S.I. Stoliarov, Thermal analysis method for measuring polymer flammability, J. ASTM Int. 3 (4) (2006) 1-18.

[41] D.W. van Krevelen, Some basic aspects of flame resistance of polymeric materials, Polymer 16(8) (1975) 615-620.

[42] X. Dai, P. Li, Y. Sui, C. Zhang, Thermal and flame-retardant properties of intrinsic flame-retardant epoxy resin containing biphenyl structures and phosphorus, Eur. Polym. J. 147 (2021) 110319.

[43] J.-Y. Kim, W.H. Lee, J.W. Suk, J.R. Potts, H. Chou, I.N. Kholmanov, R.D. Piner, J. Lee, D. Akinwande, R.S. Ruoff, Chlorination of Reduced Graphene Oxide

Enhances the Dielectric Constant of Reduced Graphene Oxide/Polymer Composites,

Adv. Mater. 25(16) (2013) 2308-2313.

[44] X. Mu, D. Wang, Y. Pan, W. Cai, L. Song, Y. Hu, A facile approach to prepare

phosphorus and nitrogen containing macromolecular covalent organic nanosheets for

enhancing flame retardancy and mechanical property of epoxy resin, Composites,

Part B 164 (2019) 390-399.

Table 1 Formulations of BD and BA resins.

Resin	Code	BMI (g)	AER (g)	DBA (g)	[a]Molar ratio
BD resins	BD-0.2	13.44	-	2.89	1:0.2
	BD-0.4	13.44	-	4.62	1:0.4
	BD-0.6	13.44	-	6.94	1:0.6
	BD-0.8	13.44	-	9.25	1:0.8
	BD-1.0	13.44	-	11.6	1:1
BA resins	BA-0.2	13.44	1.74	-	1:0.2

BA-0.4	13.44	3.48	-	1:0.4
BA-0.6	13.44	5.22	-	1:0.6
BA-0.8	13.44	6.98	-	1:0.8
BA-1.0	13.44	8.71	-	1:1

[a]The molar ratio of imide to allyl double bond.